



Rethinking the Invisible Protection against Unauthorized Image Usage in Stable Diffusion

Shengwei An, Lu Yan, Siyuan Cheng, Guangyu Shen, Kaiyuan Zhang, Qiuling Xu, Guanhong Tao, and Xiangyu Zhang, *Purdue University*

<https://www.usenix.org/conference/usenixsecurity24/presentation/an>

This paper is included in the Proceedings of the
33rd USENIX Security Symposium.

August 14-16, 2024 • Philadelphia, PA, USA

978-1-939133-44-1

Open access to the Proceedings of the
33rd USENIX Security Symposium
is sponsored by USENIX.

Rethinking the Invisible Protection against Unauthorized Image Usage in Stable Diffusion

Shengwei An*, Lu Yan*, Siyuan Cheng, Guangyu Shen,
Kaiyuan Zhang, Qiuling Xu, Guanhong Tao, Xiangyu Zhang
Purdue University

Abstract

Advancements in generative AI models like Stable Diffusion, DALL·E 2, and Midjourney have revolutionized digital creativity, enabling the generation of authentic-looking images from text and altering existing images with ease. Yet, their capacity poses significant ethical challenges, including replicating an artist’s style without consent, the creation of counterfeit images, and potential reputational damage through manipulated content. Protection techniques have emerged to combat misuse by injecting imperceptible noises into images. This paper introduces INSIGHT, a novel approach that challenges the robustness of these protections by aligning protected image features with human visual perception. By using a photo as a reference, approximating the human eye’s perspective, INSIGHT effectively neutralizes protective perturbations, enabling the generative model to recapture authentic features. Our extensive evaluation across 3 datasets and 10 protection techniques demonstrates its superiority over existing methods in overcoming protective measures, emphasizing the need for stronger safeguards in digital content generation.

1 Introduction

Generative AIs such as Stable Diffusion [26], DALL·E 2 [25], and Midjourney [9] have taken the world by storm because of their superb capability of generating authentic-looking images from only a few words. A stunning “photograph” can be captured without venturing into the wilderness to search for the perfect scene. Instead, it can be achieved by describing all the essential elements required within the scene. If one takes a photo with some flaws but is not a master of image editing tools such as Photoshop, they can simply demand the generative AIs to repair it. Generative AIs also exhibit a level of painting expertise that rivals that of the finest human artists. A breathtaking “artwork” can be made by naming the genre (e.g., the brushstroke and color palette) and describing the content to the AIs.

*Equal contribution.

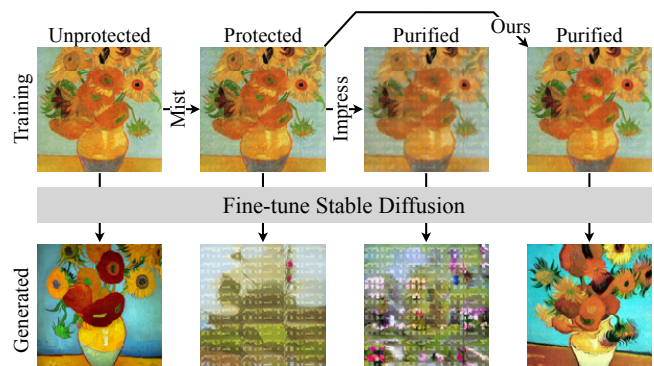


Figure 1: Examples of the existing protection and countermeasure in style mimicry attack. The existing countermeasure Impress cannot break the protection Mist, while ours can.

Beyond utilizing their generative capability learned from an enormous amount of data, a lot of fine-tuning techniques have been devised to personalize a pre-trained Stable Diffusion model [8, 28] with a small set of data (e.g. even only 5-20 images). For example, 5 photos of a person can make a Stable Diffusion model memorize that person and create photos of that person in different contexts. Several real paintings of Vincent van Gogh are sufficient to teach a Stable Diffusion model to paint like him.

These techniques have contributed to the widespread adoption of generative AIs like never before. However, they have also raised numerous serious concerns and have had a detrimental impact on many individuals and society when exploited by malicious users. A major concern is aroused from the *style mimicry attack* via a personalized Stable Diffusion model. Assume Vincent is the victim artist. He spent years working hard and learning how to paint. After he developed his unique painting style, he hoped to live a better life by selling his paintings, but still couldn’t afford more than a hand-to-mouth existence. He started to advertise and promote his paintings online to attract more customers. However, an

attacker downloaded those paintings to fine-tune a Stable Diffusion model to produce counterfeits. The image at the top left corner of Figure 1 (annotated with “Unprotected” and “Training”) denotes a real painting from Vincent used to fine-tune a Stable Diffusion model and the image below is a counterfeit generated by the model. Looking at the shape of the flowers and the vase as well as the impasto brushstrokes, one has enough confidence in believing they are both from Vincent. To make a profit, the attacker sold them at a lower price. This could completely destroy Vincent’s life and career.

Realizing these attacks, researchers make every effort to devise *protection methods* to prevent images from being misused. One of the most famous tools is Glaze [36] that added *invisible* perturbations to the painting to prevent the Stable Diffusion model from learning the correct painting style. Vincent decided to use it to protect his artwork. But shortly, he found there were new counterfeits because the recently proposed *countermeasure* Impress [3] can purify the protected images to disable the protective effect¹. Before he gave up, he found another tool Mist whose protection cannot be removed by Impress as demonstrated by the second and third columns in Figure 1. In particular, the attacker fine-tuned a Stable Diffusion model on the Mist-protected paintings but found the generated image (in the second column) was of low quality. Then the attacker tried to use Impress to purify the protected paintings before training a model on them, but the generated image (in the third column) is still chaotic. Now, Vincent is satisfied with the protection and publishes the Mist-protected paintings online.

However, is this *invisible*-perturbation-based protection really sufficient? To better answer this question, we study the inherent properties of existing protections. All of these methods are based on adding *invisible* noises [14, 15, 36, 44, 46, 49, 53], with which the models can no longer learn the correct features. The invisibility requirement is because they don’t want humans to perceive the difference between unprotected and protected images. Otherwise, the market values of the paintings may greatly degrade. In other words, these noises can only fool AI models but not humans. If we can transfer this human invisibility to the models by aligning the features of the protected images in the lens of models and the eyes of humans, the added noises would be neutralized, and the model should be able to pick up the correct features (as humans). With this insight, we propose a new approach called INSIGHT to evaluate the robustness of existing protections.

More specifically, we propose to use the photo of a protected image as the alignment reference. The photo can be considered a good approximation of human visual perception because of the similarity between the structures of the eyes and the design of a camera [23, 39, 45]. We observe the architecture of a Stable Diffusion model contains two components. Therefore we align the features of the protected image with

its reference via a contrastive loss in each component. This is achieved by finding a new perturbation to counteract the protective perturbation. The rightmost column in Figure 1 shows our approach can invalidate the protection. The attacker first uses our approach to purify the protected paintings and then fine-tune a Stable Diffusion model on them. The generated image in the second row resembles Vincent’s style again.

Besides the style mimicry attack, attackers can also create fake images of certain identities using Stable Diffusion models, including *subject recontextualization* and *image manipulation* attacks. These fake images can damage the subject’s reputation (e.g., a fake photo of the person in prison) or even cause significant financial loss. For example, fake generations made a multinational company lose more than 25 million dollars in this February [4]. Details of different attacks are in Section 2.2. *We want to emphasize that our goal is not to facilitate attacks, but to provide a tool to evaluate protections and help build stronger protections.* Our contributions are summarized as follows:

- We analyze the design space of existing protections and countermeasures (that aim to remove protections). We point out the invisible perturbation is not robust. We observe that the ineffectiveness of existing countermeasures is because they fail to constrain both components of the Stable Diffusion models and lack a good reference (to facilitate removing protective noises).
- We design a new countermeasure against protections. It exploits the invisibility of the added perturbation. It invalidates protection by aligning the features of the protected images with the human visual reference (e.g., a photo) in the two components of a Stable Diffusion model.
- We build and open-source a tool INSIGHT [21] (Rethinking the Invisible Protection against Unauthorized Image Usage in Stable Diffusion) and extensively evaluate it against 10 existing protections on three datasets. We compare our approach against 4 baselines including the SOTA Impress in 3 types of attacks (i.e., style mimicry, subject recontextualization, and image manipulation). Experimental results show our approach can outperform all baselines against all protections in all attacks. For style mimicry, our approach has 1.4x the effectiveness of the best baseline. For the other two attacks, our approach is also the most effective and can help generate images of the best quality. We also conduct human studies and GPT4-based studies. On average, users/GPT4 prefer our approach to the best baseline in 93.9%/94.2% cases. We also show the effectiveness of our approach in the commercial service.

Threat Model. We use the same threat model as the existing countermeasure [3]. The defenders want to use invisible

¹Results can be found in its original paper and our evaluation

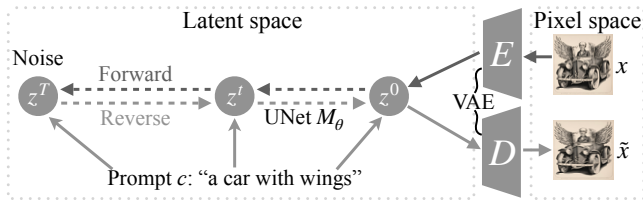


Figure 2: Architecture of the Latent Diffusion Model. We omit the text model here for simplicity.

perturbations to protect the images from being misused. The defender can utilize arbitrary image transformation methods and pre-trained diffusion models. The goal of the attackers is to diminish the protection to misuse images. They have no knowledge of the exact protection method or the corresponding clean (unprotected) images. But they have complete control over the protected images and thus can utilize countermeasures to remove protection. They can exploit pre-trained diffusion models.

Ethics. Our human study has received approval from our institutional review board (IRB). It is collected anonymously via Amazon Mechanical Turk. We don’t collect or store any personally identifiable information.

2 Latent Diffusion Model and Image Misuse

2.1 Latent Diffusion Model

Figure 2 shows the architecture of the Latent Diffusion Model (LDM) or Stable Diffusion (SD) [26]. Different from existing Diffusion Models (DM), such as the Denoising Diffusion Probabilistic Model [7] and Noise Conditional Score Network [41], that operate in the pixel domain, LDM runs the diffusion process in a compressed latent space created by a Variational Autoencoder (VAE) consisting of an encoder \mathcal{E} and a decoder \mathcal{D} [5]. \mathcal{E} encodes an image x from the pixel space into the latent space as $z^0 = \mathcal{E}(x)$ while \mathcal{D} decodes a latent vector to recover an image to the pixel space. The encoder and decoder compose the so-called first stage, while the diffusion process in the latent space is the second stage.

The forward process (e.g. z^0, z^1, \dots, z^T) in LDM iteratively adds Gaussian noises to z^0 until it becomes a Gaussian noise, that is, $z^T \sim \mathcal{N}(0, I)$. The training goal of LDM is to learn a network M_θ (usually a UNet) to form a reverse process to iteratively denoise the Gaussian noise z^T to recover z^0 according to the defined distribution:

$$z^{t-1} \sim \mathcal{N}(z^{t-1}; \frac{1}{\sqrt{\alpha^t}} \left(z^t - \frac{1 - \alpha^t}{\sqrt{1 - \bar{\alpha}^t}} M_\theta(z^t, t) \right), \sigma^t I) \quad (1)$$

where α^t is the transitional content schedulers mathematically defined in DM and $\bar{\alpha}^t = \prod_{i=1}^t \alpha^i$ [7, 26].

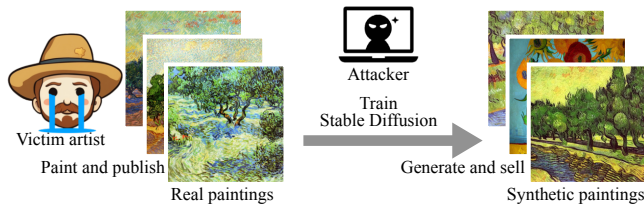


Figure 3: Style mimicry. Attackers use the victim artist’s paintings (e.g., Vincent van Gogh) to train a Stable Diffusion model to generate fake paintings in the same style.

One advantage of LDM is that it can utilize an additional condition c such as text prompts to guide the reverse process to generate the desired images². For text-to-image generation (Stable Diffusion Models), each training sample is a pair of an image x and a text prompt c . This conditional generation is usually implemented as extra attention layers in M_θ . Intuitively, the conditional training goal is to approximate the added noise $\epsilon^t \sim \mathcal{N}(0, I)$ at the t -th step, and the simplified training loss is as follows.

$$L_{\text{LDM}} = \mathbb{E}_{t, z^0, c, \epsilon^t} \|\epsilon^t - M_\theta(\sqrt{\bar{\alpha}^t} z^0 + \sqrt{1 - \bar{\alpha}^t} \epsilon^t, c, t)\|_2^2 \quad (2)$$

where t is sampled from $[1, T]$, $z^0 = \mathcal{E}(x)$, $\epsilon^t \sim \mathcal{N}(0, I)$.

After training, to generate an image for a given text prompt c , a latent vector z^T is first sampled from the Gaussian distribution and progressively denoised to get z^0 ; z^0 is further decoded by \mathcal{D} to synthesize the final image $\tilde{x} = \mathcal{D}(z^0)$.

2.2 LDM-based Image Misuse

The high capability of LDM in few-shot image generation and manipulation empowers non-experts to create amazing artwork with only a few lines of text. These fantastic models and techniques contribute to the blossom of generative AIs. However, once used by malicious attackers, they also brought a lot of concerns about image misuse. There are three main misuse scenarios. Each of them can cause severe damage.

Style Mimicry. The first type of misuse is style mimicry which has concerned a lot of researchers and artists [36]. The malicious attackers want to generate synthetic paintings with the same style as certain artists to make profits. Figure 3 provides an illustration. The victim artist (e.g., Vincent van Gogh) draws some paintings and advertises them online. After downloading them, the attackers use DreamBooth [28] to fine-tune a pre-trained Stable Diffusion model. For example, they can force the model to associate the text prompt “a [V] painting” with the victim’s painting style. They can then use this model to generate “new” paintings of Vincent as long as they insert “a [V] painting” into the prompt. Comparing the

²Another network will extract embedding of the text prompt and feed it to UNet. We omit this step here for simplicity.

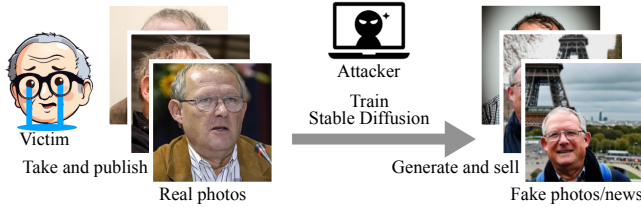


Figure 4: Subject recontextualization. Attackers use the victim’s (e.g., Adam Michnik) photos to train a Stable Diffusion model to create the victim in new contexts (e.g., Eiffel Tower).

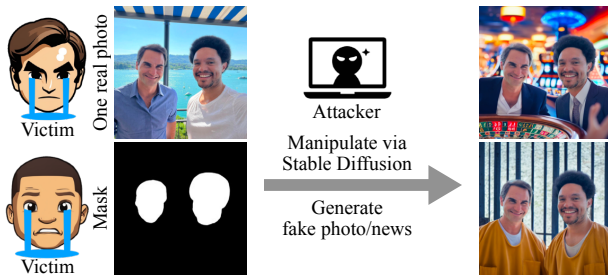


Figure 5: Image manipulation. Attackers use a Stable Diffusion model to manipulate the unmasked (dark) area of the victims’ (e.g., Roger Federer and Trevor Noah) photo.

images on the right and left in Figure 3, it looks like they were painted by the same artist. Attackers don’t need to spend years learning and practicing painting. What it takes is just a few clicks and several minutes. This can have negative impacts on artists, students, and even the whole society.

Subject Recontextualization. The Stable Diffusion model is not only able to mimic painting styles but also able to memorize subjects. This enables the second type of image misuse known as subject recontextualization as demonstrated in Figure 4. The goal of this attack is to create the subject in a new context. The created subject is usually in new poses, different facial expressions, and unseen clothes. The attackers first obtain a set of the victim’s photos. They are either taken by the attackers or retrieved from online resources. The attackers then use DreamBooth [28] to make the model connect the text prompt “a [V] person” with the victim. As a result, the attackers can generate photos of the victim in front of the Eiffel Tower using the prompt “a [V] person in front of the Eiffel Tower”. When the victim is put into some wicked context such as being in prison or arrested by the police, news with such fake high-fidelity photos can produce a catastrophe.

Single Image Manipulation. Different from the previous two, the attackers want to manipulate a *single* photo, as shown by Figure 5. They mask the photo to denote the unchanged area and ask the Stable Diffusion to repaint the other area according to the provided text [6, 32]. In this case, they don’t use a set of photos to fine-tune a Stable Diffusion model. Instead,

Table 1: Strategies of existing protection methods. Anti means Anti-DreamBooth. PG_E and PG_D mean the encoder and diffusion protection methods in PhotoGuard.

Comp.	Glaze	PG_E	PG_D	AdvDM±	SDS±	Anti.	Mist	ITA	SDST
VAE	●	●	◐	◐	◐	◐	●	●	●
UNet	○	○	◐	●	●	●	●	●	●

○ not consider ◐ implicitly consider ● explicitly consider

they use a pre-trained model to complete the manipulation. This makes the attacks easier to conduct and cause damage. Different from the previous attack, it usually preserves the same subject (e.g., the face pixels). The right two fake photos in Figure 5 are crafted using the prompts “men in casino” and “men in prison”. The high fidelity of the photos can persuade people to believe the two people are indeed in prison.

There are multiple differences between the last two types of attacks. First, subject recontextualization requires *training* a model using several images while single image manipulation utilizes a *pre-trained* model. Second, the former needs to *memorize* the subject and then *recreate* it in a new context. The created subject usually has different poses, facial expressions, and clothes from the training images. For example, Adam in the fake photo of Figure 4 is smiling, wearing a backpack, and has a smaller head size. All of these features are different from the training photos. However, image manipulation *does not memorize* anything and directly modifies the unmasked area. That is, the pixel values in the masked area are copied from the real image. For example, the two images on the right side have the same heads as the real image on the left in Figure 5.

3 Existing Protection Methods

Attacks being proposed, researchers devise different protection methods to mitigate them. They add protective perturbations δ to the original photos and publish the protected ones instead. We have seen that LDM consists of two stages/components: the VAE (\mathcal{E} and \mathcal{D}) stage, and the diffusion stage with M_θ . In the following, we briefly explain existing protection methods based on which component they explicitly target (summarized in Table 1). There are mainly two categories: 1) constraining VAE only, and 2) constraining both VAE and UNet. There is no existing protection only constraining UNet because one has to go through VAE to constrain UNet in the latent space.

Constraining VAE Only. This type of protection tries to mislead the VAE to regard the protected image $x_{\text{protected}} = x + \delta$ as a carefully selected *target image* x_{target} [30, 36] by minimizing the distance between the latent vector of x and that of x_{target} : $\delta = \text{argmin}_\delta \|\mathcal{E}(x + \delta) - \mathcal{E}(x_{\text{target}})\|_2^2$. Glaze [36] first transforms the painting into a genre different from the ground truth one (e.g., from Post Impressionism to Cubism) and uses

Table 2: Strategies of countermeasures. The first three are post-processing methods independent of diffusion models.

Comp.	JPEG	Gaussian	Crop+resize	Impress	Ours	○ not consider
VAE	○	○	○	◐	●	◐ implicitly consider
UNet	○	○	○	○	●	● explicitly consider

that as x_{target} , while the encoder protection of PhotoGuard [32] (denoted by PG_E) uses a gray image.

Constraining both VAE and UNet. We can also achieve protection by misleading the UNet. Because UNet in an LDM is defined in the latent space, constraining UNet cannot avoid considering VAE. Based on the space where the optimization loss is defined, protection of this type can be further subdivided into three categories. The first one is the diffusion protection in PhotoGuard [32] (denoted by PG_D). It defines the loss in the pixel space and thus implicitly considers the VAE and UNet. It wants the image generated by LDM based on the protected one $x_{\text{protected}} = x + \delta$ to be similar to a target image (e.g., a gray image): $\delta = \text{argmin}_{\delta} \|f_{\text{LDM}}(x + \delta) - x_{\text{target}}\|_2^2$, where f_{LDM} denotes the whole LDM generation process.

The second subdivision defines the optimization loss in the UNet component, including AdvDM+ [15], SDS± and AdvDM- [49], and Anti-DreamBooth [44]. AdvDM+ forces the UNet’s output for $x_{\text{protected}}$ to deviate from the ground truth: $\text{argmax}_{\delta} \mathbb{E}_{t, \epsilon^t} \|\epsilon^t - M_{\theta}(\sqrt{\alpha^t} z^0 + \sqrt{1 - \alpha^t} \epsilon^t, c, t)\|_2^2$. Anti-DreamBooth [44] also updates the LDM to improve the protection effect against DreamBooth [28]. SDS+ reduces the time cost and GPU memory required by AdvDM+ via approximating the gradients propagated from the UNet. SDS- and AdvDM- use a similar loss with modified directions.

The third subdivision explicitly defines the loss in the VAE component in addition to the UNet, including Mist [14], ITA [53], and SDST [49]. They want to mislead both the VAE and the UNet at the same time. Mist can be considered as AdvDM+ with PG_E. ITA also updates LDM as Anti-DreamBooth. SDST is Mist with the gradient approximation.

Perturbation Bound. To avoid destroying the original image, the protection methods bound the perturbation to ensure it’s invisible. Glaze [36] uses a *learned perceptual image patch similarity* (LPIPS) [51] regularization term to penalize large perturbation while the others clip the perturbation according to predefined distance ℓ_{∞} or ℓ_2 [14, 15, 32, 44, 49, 53].

4 Limitations of Existing Countermeasures (Against Protection Techniques)

This section discusses four existing countermeasures to the aforementioned protection methods: JPEG compression, Gaussian noise, Crop+resize and Impress [3]. They aim to nullify the protective perturbations such that the adversary

can succeed. The first three methods are based on transformations evaluated in existing literature [3, 14, 33, 44, 49, 53]. They don’t utilize any information from LDM, they constrain neither VAE nor UNet. Impress is the state-of-the-art LDM-based method against Glaze and PhotoGuard. It implicitly constrains VAE as explained later. Table 2 summarizes the used strategy of each countermeasure.

Figure 6 visualizes their performance against Mist in style mimicry and indicates that improvement is still needed. The first row shows one training sample for each case. Each column shows one type of training data to fine-tune an SD. The “Clean” column fine-tunes an SD using unprotected paintings (here they are painted by Vincent). The images generated by the fine-tuned SD model are displayed in the second and third rows. We can see the generated images and the clean paintings both feature similar choppy and expressive brushstrokes and lines. Thus without any protection, style mimicry is easy. The second column shows the result when the training paintings are protected by Mist. Because it only adds small perturbations, there is no significant visual difference between the first two images in the first row. However, the generated images (in the second column of the second and third rows) are completely destroyed and have obvious Mist patterns. This is a successful protection.

We now examine the performance of the first three transformation-based methods. JPEG compresses an image in a lossy way and has been shown to be able to remove some protection effects by researchers [3, 33]. We follow their setting and use 15 as the quality factor. We first use JPEG to compress the protected paintings and use the compressed ones to fine-tune an SD model to generate new paintings. As shown by the third column in Figure 6, it removes some protection so that the generated images start to show the similar contents as the clean ones. However, the brushstrokes and color palettes are different. Another baseline is Gaussian noise, which adds Gaussian noises to the protected image. It does not work and sometimes even strengthens the protection as indicated by the fourth column.

Crop+resize has been empirically proven by researchers to be the most effective post-processing (non-LDM-based) method of removing protection compared with JPEG compression and Gaussian perturbation [3, 14, 49]³. We follow the literature to run Crop+resize by first cropping 64 pixels in all directions around the protected 512^2 image and then resizing it back to 512^2 [14, 49]. An SD model is fine-tuned on the cropped and resized images. The results of Crop+resize are listed in the fifth column. There is some improvement as the semantic contents and some wavy brushstrokes are mostly recovered. However, we can see that the painting of flowers has obvious strange patterns and the painting in the last row lacks fine brushstrokes and uses a different color scheme. Therefore, it cannot completely remove the protection.

³Our experiments in the evaluation section also show Crop+resize outperforms JPEG compression and Gaussian noise.

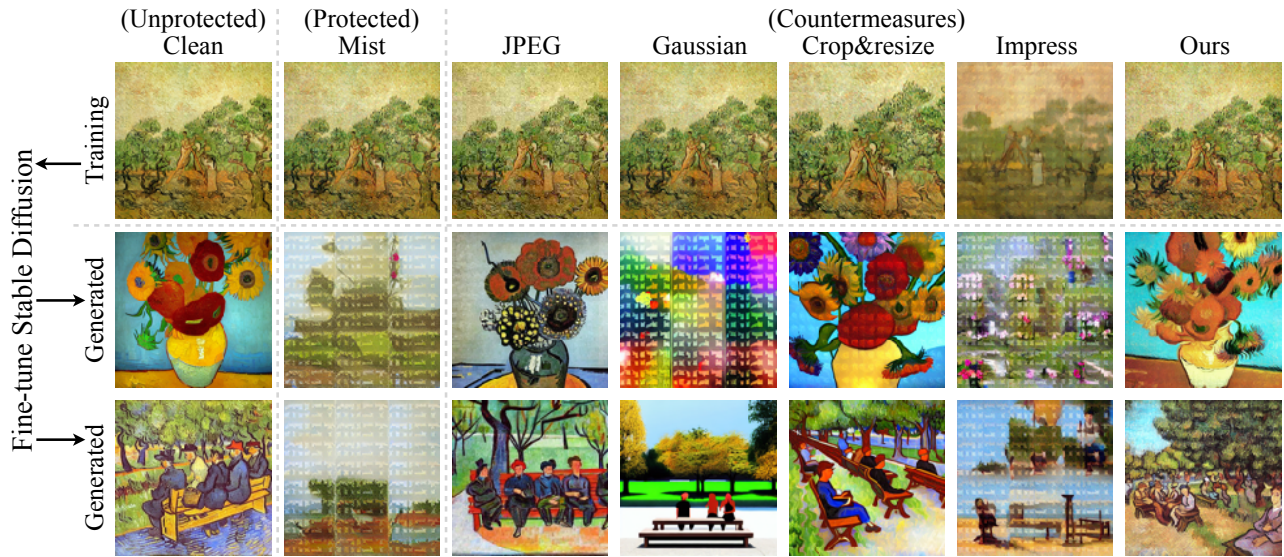


Figure 6: Examples of existing countermeasures for Mist. The first row shows samples used to train the Stable Diffusion model. The second and third rows show generated samples. Each column denotes a different setting.

Impress [3] is the SOTA countermeasure against Glaze and PhotoGuard. It observed that the image reconstructed by VAE $\mathcal{D}(\mathcal{E}(x_{\text{protected}}))$ deviates from $x_{\text{protected}}$ noticeably whereas a clean image (used in training) is close to its reconstruction, i.e., $x_{\text{clean}} \approx \mathcal{D}(\mathcal{E}(x_{\text{clean}}))$. Therefore, it proposes to remove the protection effect (in $x_{\text{protected}}$) by finding another perturbation δ such that $x_{\text{protected}} + \delta$ is close to $\mathcal{D}(\mathcal{E}(x_{\text{protected}} + \delta))$. From its optimization goal, we can see it only implicitly considers VAE but does not explicitly enforce anything inside of the VAE or UNet. The sixth column in Figure 6 lists the $x_{\text{protected}} + \delta$ in the first row. An SD is fine-tuned on the Impress-purified images. As shown by the generated images, instead of removing the protection effects, it undesirably fortifies them and the MIST pattern is more obvious now. Actually, the image processed by Impress in the first row already starts to have that pattern. Impress is effective on Glaze and PhotoGuard because the larger inconsistency produced by them can only be mitigated by removing the protection noises. However, the protection method Mist leverages a smaller inconsistency. Hence, without any other guidance, instead of removing the protection noises from $x_{\text{protected}}$, the optimization in Impress tends to inject similar noises into $x_{\text{protected}} + \delta$ to make the reconstruction consistent. As a result, Impress enhances the Mist protection instead of removing it.

As indicated by Table 1 and Table 2, different protection methods can exploit different components while existing countermeasures do not fully cover both VAE and UNet. Recall that the protection methods add invisible noises to make the protected image divert from the original one from LDM’s perspective. Because of this invisibility, we propose to craft a visual reference in the eyes of a human and use it to explicitly guide resolving the divergence produced by protection

perturbation in both VAE and UNet to overcome the shortcomings of existing countermeasures. The rightmost column in Figure 6 lists our results. The styles of the two synthetic images are very similar to the two synthetic ones in the first column since the brushstrokes and color schemes are similar, indicating our method successfully removes the protections.

5 Our Design

Our goal is to remove the protection added to $x_{\text{protected}}$ by explicitly resolving the divergence brought by the protection perturbation in both VAE and UNet. It takes a protected image $x_{\text{protected}}$ and its visual reference x_{visual} (e.g., by taking a picture of the protected image, disrupting some of the well crafted perturbations) and produces an aligned image x_{aligned} (i.e., with protection disabled to some extent). It derives the output by aligning with x_{visual} in the latent space created by VAE and the intermediate diffusion steps. Figure 7 presents an overview of the whole attack pipeline. The left part of the figure shows our optimization framework to remove the protection. The right part shows an example of style mimicry. If attackers directly train a Stable Diffusion model using $x_{\text{protected}}$, the model can only generate useless images. If attackers first use our method to remove the protection and train a model on x_{aligned} , they can fulfill the style mimicry. We will elaborate on the five crucial elements in our framework in this section: 1) visual reference x_{visual} providing guidance, 2) LPIPS loss constraining the allowed amount of changes, 3) UNet contrastive alignment explicitly utilizing the guidance as the positive direction and the protected sample as the negative direction in the UNet space, 4) VAE contrastive alignment similar to the previous one but being applied in

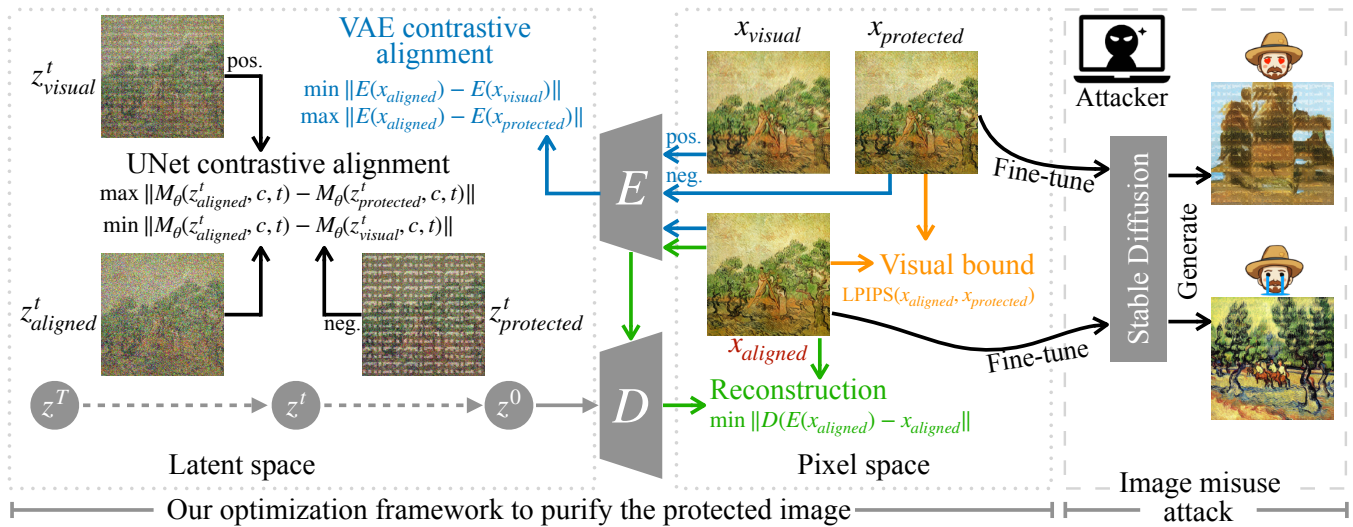


Figure 7: Overview of our pipeline. The left part shows our optimization framework that takes in a protected image and outputs an aligned (i.e., purified) one with the protection removed. The right part shows the image misuse attack (e.g., style mimicry).

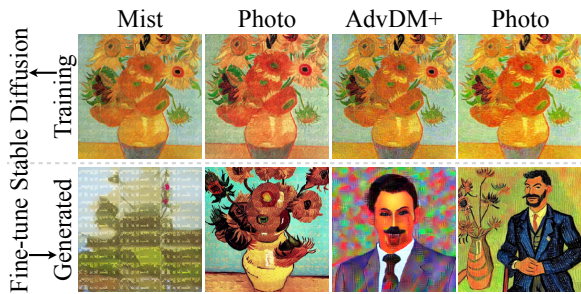


Figure 8: Cases where Photo is effective. The first/second row shows the training/generated images. The odd/even columns denote the settings of protections/photos.

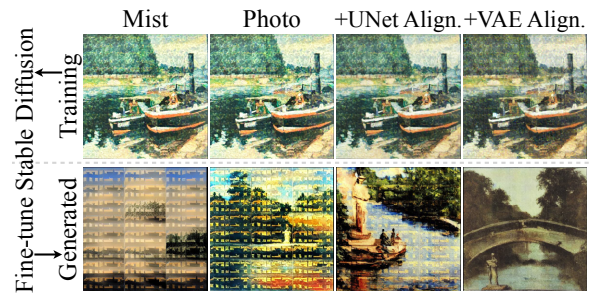


Figure 9: Effects of the UNet and VAE alignment. The first/second row shows the training/generated images. Each column denotes a different setting.

the VAE stage, and 5) reconstruction alignment reducing the inconsistent features recognized by LDM.

5.1 Visual Reference

Our intuition is that the added *invisible* noises by various protection methods only confuse the LDM but not humans. Therefore, we would like to involve such guidance to diminish the protection effect by aligning the LDM’s and human’s cognition on the protected image. To approximate what the painting looks like in human eyes, we choose to use a photo captured by the camera, since researchers consider camera can faithfully reflects humans’ visual perception [23, 39, 45]⁴.

A naive solution is to directly use this visual reference to replace the protected image in SD fine-tuning. Figure 8 shows

⁴Our evaluation also shows it outperforms other transformation-based methods.

its effectiveness. The first row shows the training images used to fine-tune the SD models. The second row shows the generated images. The first two columns show its effectiveness on Mist-protected images. The attacker wants to generate a new flower painting by mimicking Vincent’s style. The first column fine-tunes the SD model on Mist-protected images and generates images with chaotic content covered by the “MIST” pattern. In the second column, we first take photos of Mist-protected images and use them to fine-tune the SD model. The generated image draws the flowers in Vincent’s style and thus is a good mimic. The third and fourth columns show a similar case when the protection method is AdvDM+. The attackers try to generate a painting of a person in a suit. The AdvDM+ results in very strange color clusters and the Photo’s result is much better, suggesting the transformations through the physical world by taking pictures are effective in removing the digital protective noises.

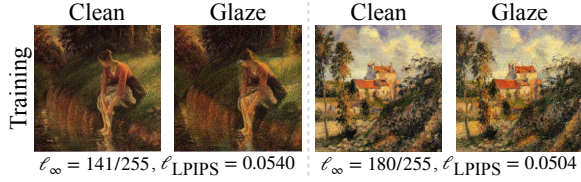


Figure 10: ℓ_∞ and ℓ_{LPIPS} between the clean *training* image and the corresponding protected *training* one. The average ℓ_∞ and ℓ_{LPIPS} on 24 random pairs are 174/255 and 0.0555.

However, it’s not sufficient in some cases as shown by the second column in Figure 9. The text prompt is “a river with a bridge and a statue”. When using Mist-protected paintings to fine-tune an SD model to generate images, there is no meaningful content. When photos are used as the training data, the general scene starts to appear. We can see the blue sky, green trees, the river, and even a statue in the middle. However, some Mist patterns are still there. This necessitates our further optimization using the reference. Note that our optimization method needs a lossy positive reference that can preserve the semantic content. We choose to use photos, but our method is not limited to working only with photos.

5.2 Visual Bound

Before starting the optimization, we need to define a way to confine the search space so that the final result is still visually similar to $x_{\text{protected}}$. This requirement is because of the invisible property of the added protective noises. Many existing works bound the perturbation in the pixel space by up to 16/255 [14, 35] or even only 4/255 [53]. This bound is not sufficient for removing the protective noises. Figure 10 shows the two pairs of a clean *training* image and the corresponding Glaze-protected one. We list the ℓ_∞ and ℓ_{LPIPS} distances between them. The ℓ_∞ of the first pair is 141/255. This bound is too large to constrain meaningful optimization in the pixel space. Because LPIPS is based on the distance between the internal features of a pre-trained network and has been shown to best match human perception, we choose to use it to constrain the visual change. More specifically, we add a regularization term during the optimization:

$$L_{\text{bound}} = \max(\ell_{\text{LPIPS}}(x_{\text{protected}} + \delta, x_{\text{protected}}) - \Delta, 0) \quad (3)$$

where Δ denotes the bound. If the optimization stays within the Δ distance, it’s 0 and adds no penalty. Otherwise, this loss penalizes the overlarge visual difference. We use the same budget 0.1 as in the literature [3].

5.3 UNet Contrastive Alignment

Note that although the photo usually cannot completely corrupt the protective noises, it must lose some of it. As such, it

can be used as a guidance for the direction of optimization, instead of the ground truth. As existing work shows the diffusion space (i.e., UNet component) corresponds to the generation of the semantic content [14, 15], we propose to use the contrastive alignment in the UNet component to pull the x_{aligned} (i.e., $x_{\text{protected}} + \delta$) in the same direction of x_{visual} and push it in the opposite direction of $x_{\text{protected}}$. More specifically, at the t -th step, we want the transition of $z_{\text{aligned}}^t \rightarrow z_{\text{aligned}}^{t-1}$ to be similar to $z_{\text{visual}}^t \rightarrow z_{\text{visual}}^{t-1}$ and different from $z_{\text{protected}}^t \rightarrow z_{\text{protected}}^{t-1}$. Similar to how the DM training loss is derived, we can encode the contrastive alignment as follows:

$$\min_{\delta} \|M_{\theta}(z_{\text{aligned}}^t, c, t) - M_{\theta}(z_{\text{visual}}^t, c, t)\|_2^2 \quad (4)$$

$$\max_{\delta} \|M_{\theta}(z_{\text{aligned}}^t, c, t) - M_{\theta}(z_{\text{protected}}^t, c, t)\|_2^2 \quad (5)$$

which can be combined into a loss:

$$L_{\text{UNet}} = \|M_{\theta}(z_{\text{aligned}}^t, c, t) - M_{\theta}(z_{\text{visual}}^t, c, t)\|_2^2 \quad (6)$$

$$- \|M_{\theta}(z_{\text{aligned}}^t, c, t) - M_{\theta}(z_{\text{protected}}^t, c, t)\|_2^2. \quad (7)$$

The image aligned with UNet contrastive loss is shown in the third column of the first row in Figure 9. This is still visually similar to the protected image because of the visual bound. After attackers fine-tune an SD model using these aligned images, they use it to generate images with a similar painting style. The third image of the second row shows the generated results. As expected, more semantic contents are restored, and we can see the trees, the river, and the statue in a clearer way. However, the textural “MIST” pattern has not been thoroughly removed. That is, the optimized result is a local optimum (i.e., an image with protective noises partially removed) instead of the global optimum. The root cause is that the guidance is only directional instead of pointy. As such, protective noises cannot be completely removed in training images and the leftover is still picked up during the training.

5.4 VAE Contrastive Alignment

The previous UNet alignment mainly covers the UNet component, while the textural pattern is usually injected via the VAE component and the resulting divergence will produce the watermark-like patterns [14, 49, 53]. More specifically, the textural protection effect is achieved by pulling the encoded feature of $x_{\text{protected}}$ to that of x_{target} by minimizing the distance between them: $\|\mathcal{E}(x_{\text{protected}}) - \mathcal{E}(x_{\text{target}})\|_2^2$. To counteract this, we propose to use the contrastive alignment in the textural space (the VAE component) to pull the $\mathcal{E}(x_{\text{aligned}})$ in the same direction of $\mathcal{E}(x_{\text{visual}})$ and push it in the opposite direction of $\mathcal{E}(x_{\text{protected}})$. Similar to the UNet contrastive alignment, our goal is:

$$\min_{\delta} \|\mathcal{E}(x_{\text{aligned}}) - \mathcal{E}(x_{\text{visual}})\|_2^2 \quad (8)$$

$$\max_{\delta} \|\mathcal{E}(x_{\text{aligned}}) - \mathcal{E}(x_{\text{protected}})\|_2^2 \quad (9)$$



Figure 11: The effect of the reconstruction loss. The first row shows the reconstructed images for the training ones in the second row. The third row shows the generated data.

which can be combined into a loss:

$$L_{\text{VAE}} = \|\mathcal{E}(x_{\text{aligned}}) - \mathcal{E}(x_{\text{visual}})\|_2^2 \quad (10)$$

$$- \|\mathcal{E}(x_{\text{aligned}}) - \mathcal{E}(x_{\text{protected}})\|_2^2. \quad (11)$$

An example of images aligned with both UNet and VAE contrastive loss is displayed in the rightmost column of the first row in Figure 9. The attackers use these aligned images to fine-tune an SD model to generate style mimics. A generated sample is shown by the fourth image of the second row in Figure 9. Now, the bridge and the statue are clearly painted without the “MIST” pattern covering the painting. The UNet alignment guides the optimization in the semantic dimension and the VAE alignment does in the textural dimension. Therefore we need both of them to fully align the final image toward the goal.

5.5 Reconstructive Alignment

The previous two constraints are defined in the latent space. The last element in our framework is reconstruction loss defined in the pixel space. This loss constrains the consistency between the aligned image and the image reconstructed through VAE. The intuition is a clean image should be close to its reconstruction, that is, $x_{\text{clean}} \approx \mathcal{D}(\mathcal{E}(x_{\text{clean}}))$. For a protected image, the reconstruction differs a lot, that is, $x_{\text{protected}} \not\approx \mathcal{D}(\mathcal{E}(x_{\text{protected}}))$. This is reflected by the first two columns of the first two rows in Figure 11. For the clean painting of an animal and a person, its reconstruction is almost the same as itself. However, for the Glaze-protected image, its reconstruction becomes two cubistic faces (highlighted by green circles). By zooming in, we can see the animal becomes a face and the upper body of the person forms the other face. The attackers use the training images in the second row to fine-tune an SD model and generate images in the third

row. The model fine-tuned on clean images generates natural paintings, while the one fine-tuned on Glaze-protected images generates images in a different Cubism style.

It’s empirically observed that this reconstruction loss has two benefits. First, the purified training image with the extra reconstruction loss is less noisy. It’s reflected by comparing the rightmost two images of the second row in Figure 11. If we compare the two images with the corresponding reconstruction, we can see the one purified with the reconstruction loss is indeed more similar to its reconstruction. Second, it can improve the quantitative metrics of the generated images. The attackers train two SD models on purified images with and without the reconstruction loss. Although the images generated by the two models have little visual difference in terms of the painting style and quality, the former gives the higher quantitative performance such as the classification accuracy of the style.

Since our goal is to minimize the difference between the purified image x_{aligned} and its reconstruction, the loss is defined as follows:

$$L_{\text{reconst.}} = \|\mathcal{D}(\mathcal{E}(x_{\text{aligned}})) - x_{\text{aligned}}\|_2^2. \quad (12)$$

The complete optimization objective of our framework is:

$$L_{\text{INSIGHT}} = \lambda_1 \cdot L_{\text{bound}} + \lambda_2 \cdot L_{\text{UNet}} + \lambda_3 \cdot L_{\text{VAE}} + \lambda_4 \cdot L_{\text{reconst.}}, \quad (13)$$

where λ ’s adjust the strength of each loss element. By default, we set them as $\lambda_{\text{bound}} = 0.1$, $\lambda_{\text{UNet}} = 0.1$, $\lambda_{\text{VAE}} = 0.1$, $\lambda_{\text{reconst.}} = 1$.

6 Evaluation

6.1 Experimental Setup

We implemented our optimization framework in PyTorch [22]. We evaluate our approach against 10 existing protection methods and reveal their vulnerability. Our experiments run on a server with Intel Xeon Silver 4214 2.20GHz 12-core CPUs with 256 GB RAM and 8 NVIDIA Quadro RTX 6000 GPUs.

Datasets and Models. We evaluate INSIGHT on three different datasets WikiArt [31], CelebA-HQ [10], and Helen [11], following the literature [3, 14, 15, 36, 44, 49, 53]. The WikiArt dataset contains 42k+ artworks from 129 artists. Each artwork is categorized into a genre (e.g., Cubism, Impressionism). We filter out artists whose paintings can be not well classified (i.e., classification accuracy < 80%) by a CLIP genre classifier [24] as the existing work [3, 36]. We then randomly select 7 artists for evaluation on style mimicry. The CelebA-HQ dataset contains 30k celebrity images. We use the same strategy as Anti-DreamBooth [44] and randomly select 10 identities with 12 images for each individual for evaluation on subject recontextualization. The Helen dataset contains 2k+

images from Flickr. Each image comes with a mask annotating the face area. We randomly select 48 pairs of images and prompts for evaluation on image manipulation. We use the same Stable Diffusion models [26] with resolution 512×512 as existing protections and countermeasures.

Generation Methods. For style mimicry and subject recontextualization, we mainly use Dreambooth. For image misuse, we use mask-based inpainting.

Protection Methods. We evaluate our approach against Glaze, AdvDM±, Mist, ITA, SDS±, Anti-DreamBooth and SDST for style mimicry, Anti-DreamBooth for subject contextualization, PhotoGuard for image manipulation. For each protection, we use its official implementation.

Baselines. As we have introduced in Section 4, we compare our approach against four baselines: JPEG compression, Gaussian noise, Crop+resize, and Impress. For the first three baselines, we use the same settings as existing works [3, 14, 53]. For Impress, we use the official implementation.

Evaluation Metrics. We use similar metrics as existing works [3, 14, 32, 36, 44, 53]. For style mimicry, we use Clip Accuracy [3, 24, 36] and Diffusion Accuracy [3, 12]⁵. For the other two attacks, we use image quality metrics including Peak Signal to Noise Ratio (PSNR), Structural Similarity Index Measure (SSIM) [47], Feature Similarity Index Metric (FSIM) [50], Visual Information Fidelity (VIFp) [37], Blind/Referenceless Image Spatial Quality Evaluator (BRISQUE) [18], and LPIPS [51]. In our scenario, for all metrics except the last two, it's the higher the better.

Clip Accuracy. A pre-trained CLIP model is used to classify the genre of a given painting. A clip model measures the text-image similarity. Given a painting, the CLIP model computes its similarity to a set of pre-defined genres and returns the most similar one.

Diffusion Accuracy. Given a painting and a potential genre, it uses the genre as the text condition and computes the reconstruction error for the painting with a Stable Diffusion model. From the set of pre-defined genres, it chooses the one with the smallest error as the label.

Image Quality Metrics. PSNR quantifies the ratio between the maximum possible signal power and the power of corrupting noise. SSIM calculates the structural similarity between two images. FSIM measures the feature similarity of two images. VIFp measures the quality of an image based on the premise of information fidelity. BRISQUE is a no-reference image quality measurement for individual images.

Anonymous Human Study. Because the audience of artworks is human, it's necessary to conduct human studies to evaluate whether our approach outperforms baselines. Figure 12 shows a question sample for style mimicry. We provide

⁵We mainly report Clip Accuracy because it's very time-consuming to compute Diffusion Accuracy. For one artist with one protection and one baseline, it needs about 30 minutes. Results for Diffusion Accuracy can be found in Appendix A.

Do you think (B) or (C) has the more similar painting styles (e.g., brushstrokes, color schemes, etc.) as the painting (A)?

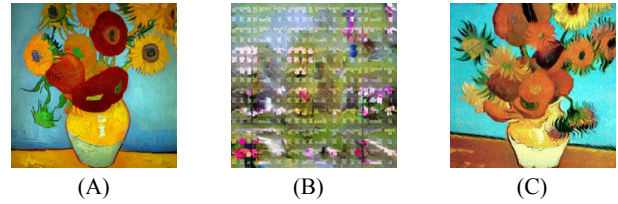


Figure 12: A human study example for style mimicry.

the user with the image generated from a model trained on clean data as (A) and images as (B) or (C) generated from a model trained on images processed by ours or a baseline. We ask the user which of (B) and (C) has a more similar painting style (e.g., brushstrokes, color schemes, etc.) as the painting (A). Question examples for subject recontextualization and image manipulation can be found in our online material [21]. Our human study focuses on Crop+resize and Impress because the former is the strongest transformation-based method while the latter is the SOTA DM-based method. For the comparison between one baseline and ours on each protection, we provide a questionnaire including 6 different multiple-choice questions. For each questionnaire, we collect the answers from 4+ users.

GPT4-based Study. We also utilize GPT4-Vision to simulate the above human study because this large multimodal model can understand images and text and has shown astonishing performance in many tasks. We ask GPT4-Vision to answer two types of questions. The first one is the relative comparison similar to those used in our human study. The second one is the pair-wise style similarity between the image generated in the clean setting and the image generated in a baseline setting or ours. We use a 5-level scale where 1 means “completely different” and 5 means “identical”. Detailed setup is explained in Appendix B.

6.2 Results on Style Mimicry

For experiments on style mimicry, we fine-tune Stable Diffusion models separately on clean data, protected data, protected data transformed by JPEG compression, Gaussian noise, or Crop+resize, protected data purified by Impress or ours. We then use the models to generate images and calculate the Clip accuracy on each set.

Overall Results. Figure 13 shows the average Clip accuracy of different settings. The x-axis denotes different protection methods except that the first “Average” group shows the average result over all protection methods. The y-axis shows the Clip accuracy. The red dashed line means the average Clip accuracy in the clean setting is about 90%. The blue bars show the accuracy of protections. On average the protection can decrease the accuracy from 90% to 35% and Mist

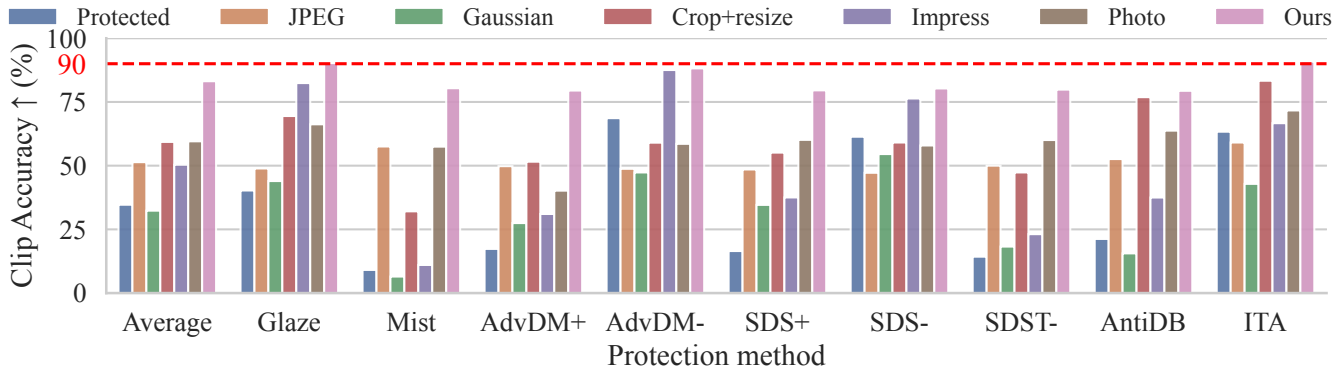


Figure 13: Clip Accuracy for images generated in different settings. The protections intend to reduce it while baselines and ours try to improve it. The red dashed line shows that the unprotected setting has an accuracy of 90%.



Figure 14: Examples of existing countermeasures for the protection method SDST-. Each row shows synthetic samples generated by the Stable Diffusion model using the same prompt. Each column denotes a different setting.

exhibits the strongest effect on decreasing it to below 10%. Among the three transformation-based methods, Crop+resize indeed is very effective in diminishing the protection. It improves the average accuracy from 35% to 59% much more than JPEG and Gaussian. As for Impress, although its average performance is slightly lower than Crop+resize, it outperforms Crop+resize by a lot of margin on Glaze, AdvDM- and SDS-. Especially on Glaze, Impress almost doubles the accuracy of the Glaze-protected one, consistent with its reported performance [3]. When trained on images purified by our approach, the Clip accuracy of the generated images gets improved by about 138%. It almost completely removes the protection effect of Glaze, AdvDM-, and ITA. On Mist-protect images, the accuracy restored by our approach is about 7.3x of Impress's and 2.5x of Crop+resize's. All these results show our approach outperforms existing baselines. Figure 14 visualizes some results. Each row shows the *generated* images by Stable Diffusion models fine-tuned on different settings. Among all the countermeasures, ours leads to the best mimicry. More visualized results are in Appendix D.

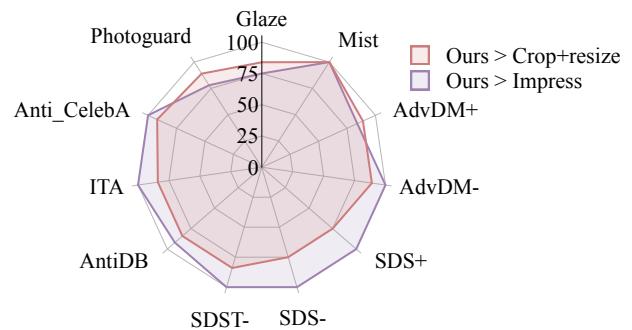


Figure 15: Human study results.

Results of Human and GPT4-based Studies. Figure 15 shows a radar chart of our human study results. Each spoke means a protection method and the length denotes how many users prefer ours to the baseline (Crop+resize in light red and Impress in light purple). A length larger than 50% means they consider ours to be better. For example, on ITA-protected

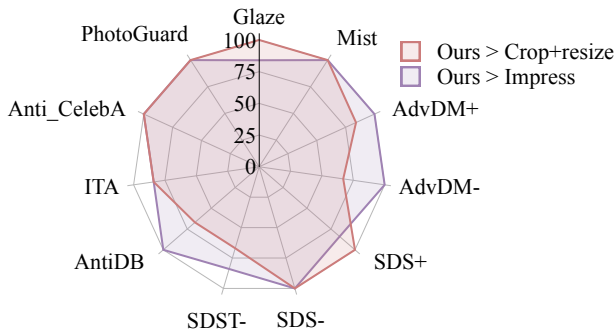


Figure 16: GPT4-Vision study results.

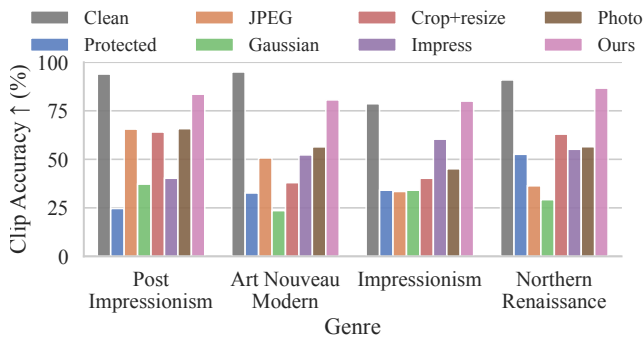


Figure 17: Clip accuracy for different genres.

images, 100% users prefer ours to Impress and 84% prefer ours to Crop+resize. Figure 16 shows the preferences of the GPT4-Vision model. On average, it prefers ours to Impress in about 94.2% cases. Table 3 shows the pair-wise similarity results. A score ≥ 3 means GPT4-Vision considers the two images to have a similar style. Ours achieves the highest average score of 3.5 while baselines’ are lower than 3.

Results on Different Genres. Figure 17 shows the results grouped by different genres averaged over different protections. The x-axis denotes four different genres: Post Impressionism, Art Nouveau Modern, Impressionism, and Northern Renaissance. The gray bar denotes the clean accuracy while bars in other colors mean the same settings as Figure 13. Among the four genres, we can see existing protections perform best for Post Impressionism. Crop+resize removes the protections more on Post Impressionism and Northern Renaissance than the other two genres. Impress has a better effect on Impressionism than other genres. Our approach outperforms baselines in all genres and is slightly more effective in Northern Renaissance than other genres.

6.3 Results on Subject Recontextualization

Table 4 list image quality metrics in subject recontextualization. For FSIM/SSIM/PSNR/VIFp/LPIPS, we compute the

Table 3: Pair-wise similarity results via GPT4-Vision.

Method	Avg.	Glaze	Mist	AdvDM+/-	SDS+/-	SDST-	AntiDB	ITA
Crop&re.	2.6	3.3	2.7	2.0/2.3	2.2/2.3	2.3	3.0	3.0
Impress	2.3	4.2	1.7	2.0/2.0	2.0/2.3	1.8	2.3	2.7
Ours	3.5	4.2	3.5	3.5/3.5	3.3/3.2	3.0	4.5	3.2

Table 4: Subject recontextualization performances.

Metric	Protected	Countermeasures				
		JPEG	Gaussian	Crop&re.	Impress	Ours
FSIM \uparrow	0.5374	0.5501	0.5384	0.5500	0.5479	0.5509
SSIM \uparrow	0.1403	0.1614	0.1392	0.1615	0.1485	0.1781
PSNR \uparrow	7.7697	7.7489	7.7602	8.0172	8.0166	8.0453
VIFp \uparrow	0.0154	0.0196	0.0156	0.0173	0.0151	0.0160
BRIS. \downarrow	19.3056	23.4289	19.5316	26.4428	20.2725	18.9324
LPIPS \downarrow	0.7567	0.7466	0.7560	0.7343	0.7459	0.7429

average pair-wise scores between a set of images generated with clean training data and those with protected or purified ones. A larger value means the generated images are similar to those in the unprotected setting. For BRISQUE, we compute the average score directly on the generated images in each setting. A smaller value means a better image quality. Our approach achieves the best scores except for VIFp (the third best) and LPIPS (the second best) where ours still outperforms the SOTA DM-based Impress. Visualized results can be found in our online material [21].

6.4 Results on Image Manipulation

Table 5 presents the quantitative results. We compute the image quality metrics FSIM/SSIM/PSNR/VIFp/LPIPS between the image manipulated from the clean one and that from the other setting (i.e., either protected or purified). A larger value means the image is more similar to its clean counterpart. Our approach achieves the best scores on FSIM/PSNR/VIFp/LPIPS and the second best on SSIM. This means the image edited from our aligned image is more similar to the clean version than the baselines. The effectiveness of simple transformations against PhotoGuard is consistent with existing papers [3, 32, 33]. We also report the BRISQUE. A smaller BRISQUE value means a better image quality. Thus, images generated using our purified data have better quality. Figure 18 visualizes some manipulated images.

6.5 Results on the Commercial Service

Scenario [34] is a commercial service on generative AI. Users can upload a set of paintings and build a diffusion model to generate new paintings in the same style (i.e., style mimicry). We upload Mist-protected images and the corresponding images purified by our methods to obtain two diffusion models.

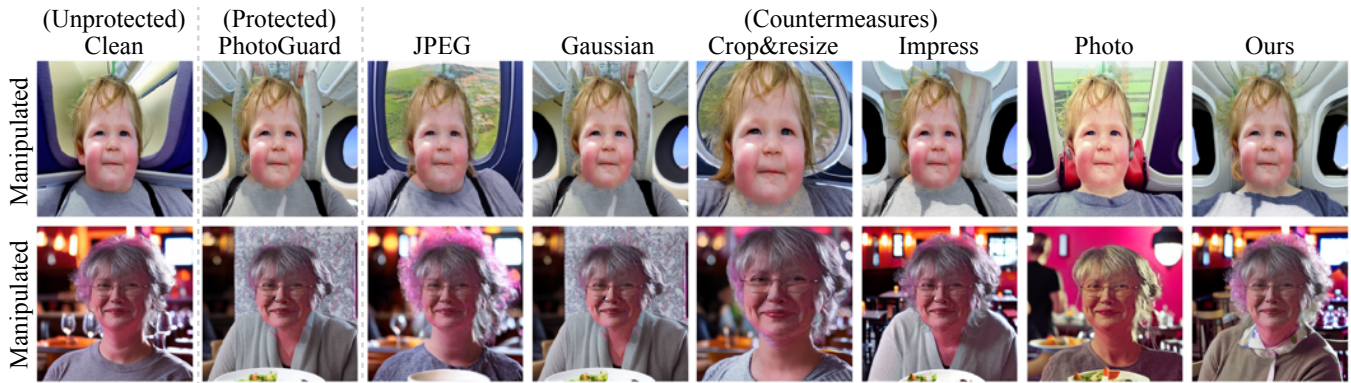


Figure 18: Examples of existing countermeasures for protection against image manipulation.

Table 5: Image manipulation performances.

Metric	Protected	Countermeasures				
		JPEG	Gaussian	Crop&re.	Impress	Ours
FSIM \uparrow	0.6879	0.7554	0.6879	0.6605	0.7422	0.7576
SSIM \uparrow	0.5086	0.6098	0.5086	0.3503	0.5610	0.6070
PSNR \uparrow	14.1296	16.4045	14.1296	12.8204	15.7630	16.4084
VIFp \uparrow	0.1811	0.2055	0.1811	0.0846	0.1677	0.2104
BRIS \downarrow	5.8796	21.4199	5.8796	11.1179	3.9056	2.8570
LPIPS \downarrow	0.5645	0.5075	0.5645	0.5970	0.5113	0.4832

We then generate new images using the two models. Figure 19 shows the results. The first row shows the images generated on the model trained on Mist-protected images are meaningless. The result in the second row demonstrates our approach can remove the protection.

6.6 Other Experiments

Because of the space limit, we put other experimental results in the appendix. Appendix C studies the adaptive protections where the defenders know our countermeasure. The effect of different fine-tuning strategies, the ablation study of our approach, our performance against GAN-based methods, and the overhead are presented in our online material [21].

7 Related Work

Diffusion Models for Image Generation Diffusion models [7, 26, 41–43] have made notable advances in image synthesis, including unconditional image generation [20, 40], text-to-image synthesis [27, 30, 38], image-to-image translation and editing [13, 29, 46, 48, 52], image inpainting [2, 16] and editing [1, 17]. Many techniques have been proposed to personalize (i.e., fine-tune) LDMs to generate desired images [8, 19, 28].

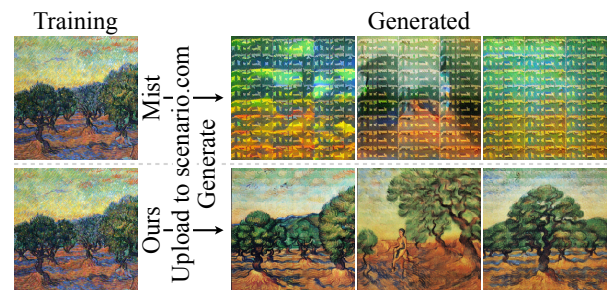


Figure 19: Mist results on the Scenario commercial service .

Protections and Countermeasures. Lots of methods have been proposed to utilize invisible perturbation to protect the images from unauthorized use [14, 15, 32, 36, 44, 49, 53]. Researchers have devised countermeasures and reported PhotoGuard and Glaze are not very robust [3, 33]. We observed that they cannot break other protections, which may provide a fake sense of safety. We design a stronger countermeasure to reveal the vulnerability of all existing protections.

8 Conclusion

Diffusion models, notable for their high-quality image generation and editing capabilities, have changed the way to create digital artwork. However, their potential for unauthorized or harmful image generation raises significant concerns. To address this, researchers have devised various image protection techniques based on invisible perturbations to prevent diffusion models from learning useful features from the protected images. This paper demonstrates that attackers can circumvent such protections by employing semantic and textual contrastive alignment with visual references, such as photos. Our experiments reveal that our method, INSIGHT, outperforms basic countermeasures like Crop+resize and the state-of-the-art DM-based method Impress.

Acknowledgments

We thank the anonymous reviewers for their constructive comments. We are grateful to the Center for AI Safety for providing computational resources. This research was supported, in part by IARPA TrojAI W911NF-19-S-0012, NSF 1901242 and 1910300, ONR N000141712045, N000141410468 and N000141712947. Any opinions, findings, and conclusions in this paper are those of the authors only and do not necessarily reflect the views of our sponsors.

References

- [1] Omri Avrahami, Ohad Fried, and Dani Lischinski. Blended latent diffusion. *ACM Transactions on Graphics (TOG)*, 42(4):1–11, 2023.
- [2] Aurélie Bugeau and Marcelo Bertalmio. Combining texture synthesis and diffusion for image inpainting. In *VISAPP 2009-Proceedings of the Fourth International Conference on Computer Vision Theory and Applications*, pages 26–33, 2009.
- [3] Bochuan Cao, Changjiang Li, Ting Wang, Jinyuan Jia, Bo Li, and Jinghui Chen. Impress: Evaluating the resilience of imperceptible perturbations against unauthorized data usage in diffusion-based generative ai. In *Thirty-seventh Conference on Neural Information Processing Systems*, 2023.
- [4] CNN News. <https://www.cnn.com/2024/02/04/asia/deepfake-cfo-scam-hong-kong-intl-hnk/index.html>.
- [5] Patrick Esser, Robin Rombach, and Bjorn Ommer. Taming transformers for high-resolution image synthesis. In *2021 IEEE/CVF Conference on Computer Vision and Pattern Recognition (CVPR)*. IEEE, June 2021.
- [6] Weixi Feng, Xuehai He, Tsu-Jui Fu, Varun Jampani, Arjun Reddy Akula, Pradyumna Narayana, Sugato Basu, Xin Eric Wang, and William Yang Wang. Training-free structured diffusion guidance for compositional text-to-image synthesis. In *The Eleventh International Conference on Learning Representations*, 2022.
- [7] Jonathan Ho, Ajay Jain, and Pieter Abbeel. Denoising diffusion probabilistic models. *NeurIPS*, 33:6840–6851, 2020.
- [8] Edward J Hu, Yelong Shen, Phillip Wallis, Zeyuan Allen-Zhu, Yuanzhi Li, Shean Wang, Lu Wang, and Weizhu Chen. Lora: Low-rank adaptation of large language models. *arXiv preprint arXiv:2106.09685*, 2021.
- [9] N Iwanenko. Midjourney v4: an incredible new version of the ai image generator, 2022.
- [10] Tero Karras, Timo Aila, Samuli Laine, and Jaakko Lehtinen. Progressive growing of gans for improved quality, stability, and variation. *arXiv preprint arXiv:1710.10196*, 2017.
- [11] Vuong Le, Jonathan Brandt, Zhe Lin, Lubomir Bourdev, and Thomas S Huang. Interactive facial feature localization. In *Computer Vision—ECCV 2012: 12th European Conference on Computer Vision, Florence, Italy, October 7–13, 2012, Proceedings, Part III 12*, pages 679–692. Springer, 2012.
- [12] Alexander C. Li, Mihir Prabhudesai, Shivam Duggal, Ellis Brown, and Deepak Pathak. Your diffusion model is secretly a zero-shot classifier. In *2023 IEEE/CVF International Conference on Computer Vision (ICCV)*. IEEE, October 2023.
- [13] Changjiang Li, Li Wang, Shouling Ji, Xuhong Zhang, Zhaohan Xi, Shanqing Guo, and Ting Wang. Seeing is living? rethinking the security of facial liveness verification in the deepfake era. In *31st USENIX Security Symposium (USENIX Security 22)*, pages 2673–2690, 2022.
- [14] Chumeng Liang and Xiaoyu Wu. Mist: Towards improved adversarial examples for diffusion models. *arXiv preprint arXiv:2305.12683*, 2023.
- [15] Chumeng Liang, Xiaoyu Wu, Yang Hua, Jiaru Zhang, Yiming Xue, Tao Song, Zhengui Xue, Ruhui Ma, and Haibing Guan. Adversarial example does good: Preventing painting imitation from diffusion models via adversarial examples. In *International Conference on Machine Learning*, pages 20763–20786. PMLR, 2023.
- [16] Andreas Lugmayr, Martin Danelljan, Andres Romero, Fisher Yu, Radu Timofte, and Luc Van Gool. Repaint: Inpainting using denoising diffusion probabilistic models. In *Proceedings of the IEEE/CVF Conference on Computer Vision and Pattern Recognition*, pages 11461–11471, 2022.
- [17] Chenlin Meng, Yutong He, Yang Song, Jiaming Song, Jiajun Wu, Jun-Yan Zhu, and Stefano Ermon. Sdedit: Guided image synthesis and editing with stochastic differential equations. *arXiv preprint arXiv:2108.01073*, 2021.
- [18] Anish Mittal, Anush Krishna Moorthy, and Alan Conrad Bovik. No-reference image quality assessment in the spatial domain. *IEEE Transactions on Image Processing*, 21(12):4695–4708, 2012.
- [19] Ron Mokady, Amir Hertz, Kfir Aberman, Yael Pritch, and Daniel Cohen-Or. Null-text inversion for editing real images using guided diffusion models. In *Proceedings*

of the *IEEE/CVF Conference on Computer Vision and Pattern Recognition*, pages 6038–6047, 2023.

- [20] Alexander Quinn Nichol and Prafulla Dhariwal. Improved denoising diffusion probabilistic models. In *International Conference on Machine Learning*, pages 8162–8171. PMLR, 2021.
- [21] Our Insight. <https://github.com/njuaplusplus/Insight>.
- [22] Adam Paszke, Sam Gross, Francisco Massa, Adam Lerer, James Bradbury, Gregory Chanan, Trevor Killeen, Zeming Lin, Natalia Gimelshein, Luca Antiga, Alban Desmaison, Andreas Kopf, Edward Yang, Zachary DeVito, Martin Raison, Alykhan Tejani, Sasank Chilamkurthy, Benoit Steiner, Lu Fang, Junjie Bai, and Soumith Chintala. Pytorch: An imperative style, high-performance deep learning library. In *NeurIPS*, pages 8024–8035. 2019.
- [23] Physics lecture demonstrations at boston university. https://physics.bu.edu/~duffy/semester2/c29_eye.html.
- [24] Alec Radford, Jong Wook Kim, Chris Hallacy, Aditya Ramesh, Gabriel Goh, Sandhini Agarwal, Girish Sastry, Amanda Askell, Pamela Mishkin, Jack Clark, Gretchen Krueger, and Ilya Sutskever. Learning transferable visual models from natural language supervision. In Marina Meila and Tong Zhang, editors, *Proceedings of the 38th International Conference on Machine Learning, ICML 2021, 18-24 July 2021, Virtual Event*, volume 139 of *Proceedings of Machine Learning Research*, pages 8748–8763. PMLR, 2021.
- [25] Aditya Ramesh, Prafulla Dhariwal, Alex Nichol, Casey Chu, and Mark Chen. Hierarchical text-conditional image generation with clip latents. *arXiv preprint arXiv:2204.06125*, 1(2):3, 2022.
- [26] Robin Rombach, Andreas Blattmann, Dominik Lorenz, Patrick Esser, and Björn Ommer. High-resolution image synthesis with latent diffusion models. In *CVPR*, pages 10684–10695, June 2022.
- [27] Robin Rombach, Andreas Blattmann, and Björn Ommer. Text-guided synthesis of artistic images with retrieval-augmented diffusion models. *arXiv preprint arXiv:2207.13038*, 2022.
- [28] Nataniel Ruiz, Yuanzhen Li, Varun Jampani, Yael Pritch, Michael Rubinstein, and Kfir Aberman. Dreambooth: Fine tuning text-to-image diffusion models for subject-driven generation. In *2023 IEEE/CVF Conference on Computer Vision and Pattern Recognition (CVPR)*. IEEE, June 2023.
- [29] Chitwan Saharia, William Chan, Huiwen Chang, Chris Lee, Jonathan Ho, Tim Salimans, David Fleet, and Mohammad Norouzi. Palette: Image-to-image diffusion models. In *ACM SIGGRAPH 2022 Conference Proceedings*, pages 1–10, 2022.
- [30] Chitwan Saharia, William Chan, Saurabh Saxena, Lala Li, Jay Whang, Emily L Denton, Kamyar Ghasemipour, Raphael Gontijo Lopes, Burcu Karagol Ayan, Tim Salimans, et al. Photorealistic text-to-image diffusion models with deep language understanding. *Advances in Neural Information Processing Systems*, 35:36479–36494, 2022.
- [31] Babak Saleh and Ahmed Elgammal. Large-scale classification of fine-art paintings: Learning the right metric on the right feature. *arXiv preprint arXiv:1505.00855*, 2015.
- [32] Hadi Salman, Alaa Khaddaj, Guillaume Leclerc, Andrew Ilyas, and Aleksander Mądry. Raising the cost of malicious ai-powered image editing. In *Proceedings of the 40th International Conference on Machine Learning, ICML’23*. JMLR.org, 2023.
- [33] Pedro Sandoval-Segura, Jonas Geiping, and Tom Goldstein. Jpeg compressed images can bypass protections against ai editing. *arXiv preprint arXiv:2304.02234*, 2023.
- [34] Scenario. <https://www.scenario.com/>.
- [35] Ali Shafahi, Mahyar Najibi, Mohammad Amin Ghiasi, Zheng Xu, John Dickerson, Christoph Studer, Larry S Davis, Gavin Taylor, and Tom Goldstein. Adversarial training for free! In H. Wallach, H. Larochelle, A. Beygelzimer, F. d’Alché-Buc, E. Fox, and R. Garnett, editors, *Advances in Neural Information Processing Systems*, volume 32. Curran Associates, Inc., 2019.
- [36] Shawn Shan, Jenna Cryan, Emily Wenger, Haitao Zheng, Rana Hanocka, and Ben Y. Zhao. Glaze: protecting artists from style mimicry by text-to-image models. In *Proceedings of the 32nd USENIX Conference on Security Symposium, SEC ’23, USA*, 2023. USENIX Association.
- [37] H.R. Sheikh and A.C. Bovik. Image information and visual quality. *IEEE Transactions on Image Processing*, 15(2):430–444, 2006.
- [38] Jie Shi, Chenfei Wu, Jian Liang, Xiang Liu, and Nan Duan. Divae: Photorealistic images synthesis with denoising diffusion decoder. *arXiv preprint arXiv:2206.00386*, 2022.
- [39] Orit Skorka and Dileepan Joseph. Toward a digital camera to rival the human eye. *Journal of Electronic Imaging*, 20(3):033009–033009, 2011.

- [40] Jiaming Song, Chenlin Meng, and Stefano Ermon. Denoising diffusion implicit models. *arXiv preprint arXiv:2010.02502*, 2020.
- [41] Yang Song and Stefano Ermon. Generative modeling by estimating gradients of the data distribution. *NeurIPS*, 32, 2019.
- [42] Yang Song and Stefano Ermon. Improved techniques for training score-based generative models. In *NeurIPS*, 2020.
- [43] Yang Song, Jascha Sohl-Dickstein, Diederik P. Kingma, Abhishek Kumar, Stefano Ermon, and Ben Poole. Score-based generative modeling through stochastic differential equations. In *ICLR*, 2021.
- [44] Thanh Van Le, Hao Phung, Thuan Hoang Nguyen, Quan Dao, Ngoc N. Tran, and Anh Tran. Anti-dreambooth: Protecting users from personalized text-to-image synthesis. In *2023 IEEE/CVF International Conference on Computer Vision (ICCV)*. IEEE, October 2023.
- [45] George Wald. Eye and camera. *Scientific American*, 183(2):32–41, 1950.
- [46] Tengfei Wang, Ting Zhang, Bo Zhang, Hao Ouyang, Dong Chen, Qifeng Chen, and Fang Wen. Pretraining is all you need for image-to-image translation. *arXiv preprint arXiv:2205.12952*, 2022.
- [47] Zhou Wang, A.C. Bovik, H.R. Sheikh, and E.P. Simoncelli. Image quality assessment: from error visibility to structural similarity. *IEEE Transactions on Image Processing*, 13(4):600–612, 2004.
- [48] Julia Wollleb, Robin Sandkühler, Florentin Bieder, and Philippe C Cattin. The swiss army knife for image-to-image translation: Multi-task diffusion models. *arXiv preprint arXiv:2204.02641*, 2022.
- [49] Haotian Xue, Chumeng Liang, Xiaoyu Wu, and Yongxin Chen. Toward effective protection against diffusion based mimicry through score distillation. *arXiv preprint arXiv:2311.12832*, 2023.
- [50] Lin Zhang, Lei Zhang, Xuanqin Mou, and David Zhang. Fsim: A feature similarity index for image quality assessment. *IEEE Transactions on Image Processing*, 20(8):2378–2386, 2011.
- [51] Richard Zhang, Phillip Isola, Alexei A Efros, Eli Shechtman, and Oliver Wang. The unreasonable effectiveness of deep features as a perceptual metric. In *Proceedings of the IEEE Conference on Computer Vision and Pattern Recognition (CVPR)*, pages 586–595, 2018.
- [52] Min Zhao, Fan Bao, Chongxuan Li, and Jun Zhu. Egsde: Unpaired image-to-image translation via energy-guided stochastic differential equations. *Advances in Neural Information Processing Systems*, 35:3609–3623, 2022.
- [53] Boyang Zheng, Chumeng Liang, Xiaoyu Wu, and Yan Liu. Understanding and improving adversarial attacks on latent diffusion model. *arXiv e-prints*, pages arXiv–2310, 2023.

Appendix

A Diffusion Accuracy

Because computing Diffusion accuracy is very time-consuming, here we only display the results of different countermeasures against Glaze in Figure 20 and show the comparison is similar to Clip Accuracy and ours is still the best.

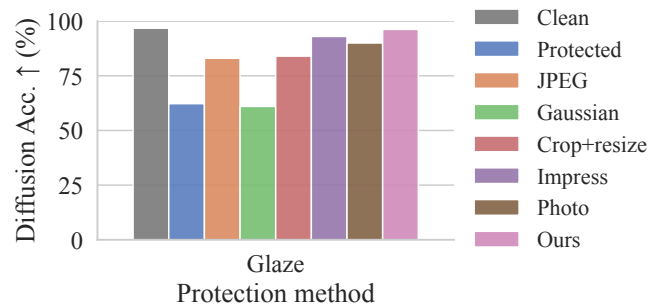


Figure 20: Diffusion accuracy on Glaze.

B Setup for GPT4-based Study

Figure 21 shows an example of our GPT4-based study. The left part lists the instructions and three images we provided for the GPT4-Vision model. In this case, the first image is generated from a model trained on unprotected paintings while the second and third images are generated from a model trained on images purified by ours and Crop+resize respectively. The right part presents its output. It considers the second image (ours) to have the same style as the first image. It also provides a step-by-step analysis. We highlight some sentences we think are the key reasons for this decision. In particular, it correctly infers “The second painting’s style seems to share the *Post-Impressionist* traits evident in the first painting”. For the example of the pair-wise comparison, please refer to our online material [21].

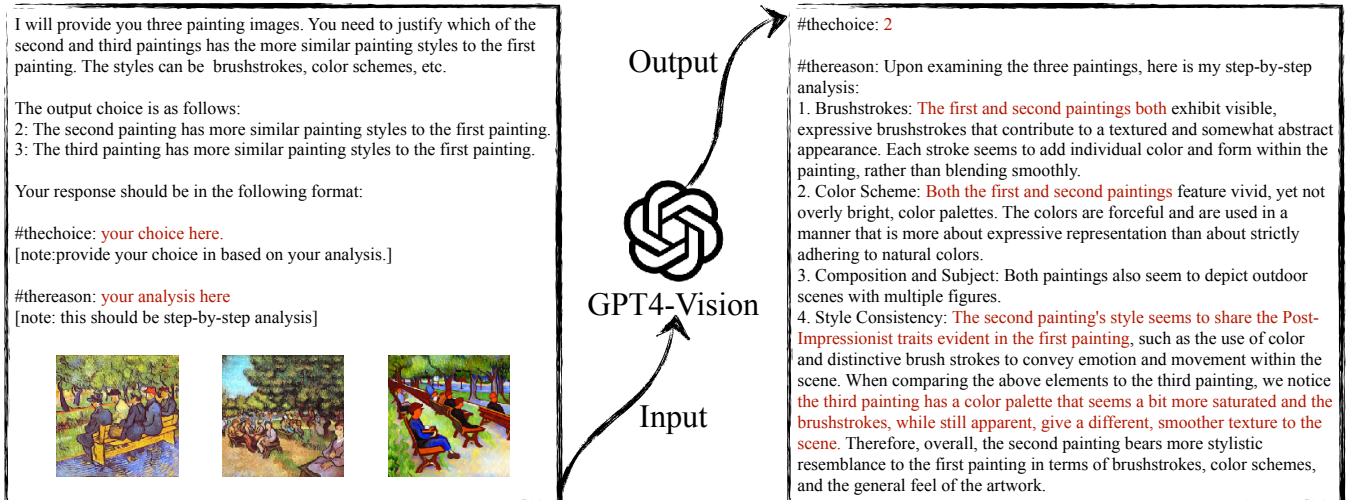


Figure 21: Example of our GPT4-based study.

Table 6: INSIGHT remains effective in purifying adaptive protections in the style mimicry scenario.

Artist	Adaptive protection		Ours purification	
	Clip Acc	Diffusion Acc	Clip Acc	Diffusion Acc
Vincent	66%	56%	89%	98%
Raphael	78%	83%	85%	97%

Table 7: INSIGHT remains effective in purifying adaptive protections under the image manipulation setting.

	FSIM \uparrow	SSIM \uparrow	PSNR \uparrow	VIFp \uparrow	BRIS. \downarrow
Protection	0.6476	0.4750	12.8395	0.1724	5.1325
Ours	0.7329	0.5674	15.0186	0.1869	1.5990

C Adaptive Protection

In this section, we aim to demonstrate the robustness of our purification method against adaptive protection. We hypothesize that attackers attempting to bypass our purification must contend with several regularization terms imposed by our proposed losses.

Firstly, the perturbations introduced by attackers must be subtle enough that the perceptual similarity (as measured by LPIPS) between the protected and original images remains within a threshold. Secondly, images generated from the protected versions should exhibit a close resemblance to those produced using visual references, indicating that perturbations must preserve the efficacy within the visual references throughout the diffusion process. Thirdly, the latent features of the protected image align with those of the visual reference (i.e., the reference’s effectiveness mirrors that of the protected image), while simultaneously presenting sufficient distinction

from the original image. Lastly, the protected images should be capable of reconstruction after the diffusion process.

Take Mist as an example, now the attacker’s optimization goal becomes:

$$\begin{aligned}
 \delta^* = \operatorname{argmin}_{\delta} & -w\mathbb{E}_{x_{\text{protected}}} \mathcal{L}_{DM}(x_{\text{protected}}, \theta) \\
 & + \|\mathcal{E}(x_{\text{target}}) - \mathcal{E}(x + \delta)\|_2 \\
 & + \lambda_1 \cdot \max(\mathcal{L}_{LPIPS}(x + \delta, x) - \Delta, 0) \\
 & + \lambda_2 \cdot \|M_{\theta}(z'_{x+\delta}, c, t) - M_{\theta}(z'_{x_{\text{visual}}}, c, t)\|_2, \\
 & + \lambda_3 \cdot (\|\mathcal{E}(x + \delta) - \mathcal{E}(x_{\text{visual}})\|_2 - \|\mathcal{E}(x + \delta) - \mathcal{E}(x)\|_2) \\
 & + \lambda_4 \cdot \|\mathcal{D}(\mathcal{E}(x + \delta)) - x + \delta\|_2^2
 \end{aligned} \tag{14}$$

Since it is challenging to create a visual reference, e.g., a photo, in every optimization step, we add Gaussian noise to the original image as the surrogate visual reference. Following Mist, we adopt the kernel size 1×1 and sigma 8×8 .

In our experimental setup, we operate under the strong assumption that attackers have full knowledge of our hyperparameters. Table 6 shows the results of the adaptive protection of Glaze on Vincent van Gogh and Raphael Kirchner’s works.

We also examine the adaptive protection under the single image manipulation setting using PhotoGuard. The results are shown in Table 7, suggesting the efficacy of INSIGHT against PhotoGuard’s adaptive protection.

We can therefore conclude INSIGHT remain effective in purifying adaptive protections.

D More Visualized Results

Figures 22 and 23 present more visualized results for different protections. More results are in our online material [21].



Figure 22: Examples of existing countermeasures for the protection method Mist. Each row shows synthetic samples generated by the Stable Diffusion model using the same prompt. Each column denotes a different setting.



Figure 23: Examples of existing countermeasures for the protection method Glaze. Each row shows synthetic samples generated by the Stable Diffusion model using the same prompt. Each column denotes a different setting.